

Global Dynamics of a Vibro-Impact Energy Harvester

Zhenbang Cao^{1,2,3,†}, Haotong Ma^{1,2,3,*}, Xuegang Yu^{1,2,3,†}, Jianliang Shi^{1,2,3}, Hu Yang^{1,2,3,*}, Yi Tan^{1,2,3} and Ge Ren^{1,2,3}

¹ Key Laboratory of Optical Engineering, Chinese Academy of Sciences, Chengdu 610209, China; caozhenbang2015@163.com (Z.C.); yuxuegang@aliyun.com (X.Y.); shijl2009@sina.com (J.S.); tanyjustc@163.com (Y.T.); renga@ioe.ac.cn (G.R.)

² The Institute of Optics and Electronics, Chinese Academy of Sciences, Chengdu 610209, China

³ University of Chinese Academy of Sciences, Beijing 100039, China

* Correspondence: mahaotong@163.com (H.M.); yangh@ioe.cn (H.Y.)

† These authors contributed equally to this work and should be considered co-first authors.

Abstract: In this paper, we consider a two-sided vibro-impact energy harvester described as a forced cylindrical capsule inclined at a horizontal angle, and the motion of the ball inside the capsule follows from the impacts with the capsule ends and gravity. Two distinct cases of dynamical behavior are investigated: the nondissipative and dissipative cases, where the dissipation is given by a restitution coefficient of impacts. We show that the dynamics of the system are described by the use of a 2D implicit map written in terms of the variables' energy and time when the ball leaves the moving capsule ends. More precisely, in the nondissipative case, we analytically show that this map is area-preserving and the existence of invariant curves for some rotation number with Markoff constant type is proved according to Moser's twist theorem in high energy. The existence of invariant curves implies that the kinetic energy of the ball is always bounded, and hence, the structure of system is not destroyed by the impacts of the ball. Furthermore, by numerical analysis we also show that the dynamical behavior of this system is regular, mainly containing periodic points, invariant curves and Aubry–Mather sets. After introducing dissipation, the dissipation destroys the regular dynamical behavior of the nondissipative case, and a periodic point with low energy is generated.

Keywords: energy harvester; vibro-impact system; invariant curves; global dynamics



Citation: Cao, Z.; Ma, H.; Yu, M.; Shi, J.; Yang, H.; Tan, Y.; Ren, G. Global Dynamics of a Vibro-Impact Energy Harvester. *Mathematics* **2022**, *10*, 472. <https://doi.org/10.3390/math10030472>

Academic Editor: Jan Awrejcewicz

Received: 22 December 2021

Accepted: 24 January 2022

Published: 1 February 2022

Publisher's Note: MDPI stays neutral with regard to jurisdictional claims in published maps and institutional affiliations.



Copyright: © 2022 by the authors. Licensee MDPI, Basel, Switzerland. This article is an open access article distributed under the terms and conditions of the Creative Commons Attribution (CC BY) license (<https://creativecommons.org/licenses/by/4.0/>).

1. Introduction

Energy harvesting (EH) refers to the process of converting various renewable energy sources such as wind, solar, wave, and vibration into electrical energy, which usually can be used to complement and substitute other sources of energy [1]. In recent years, a number of well-known conventional transduction methods of converting various energy into electrical energy were explored and developed, including piezoelectric [2], electromagnetic [3], electrostatic [4], and triboelectric [5].

To efficiently capture energy, various mechanical systems and energy conversion methods based on single-degree-of-freedom and multiple-degrees-of-freedom were developed. Linear systems are generally not suitable as EH devices under excitation with varying frequencies, since the high-power output required by the system can only be achieved by near resonance, leading to reliability and fatigue issues [6,7]. Due to these limitations, parametric excitation and nonlinearities are often introduced into systems to improve their performance and amplify their response [8–10]. In addition, due to the high efficiency of EH, multistable equilibria systems became increasingly popular in various realistic applications [11–13]. The study of vibro-impact (VI) systems for EH and the benefits of exploiting their dynamical behavior were proposed in [14,15]. The study of VI systems is both challenging and fascinating to scientists for two main reasons. The first one is that the simplest VI system has extremely complicated dynamical behavior. The best way to explain this behavior is

with the impact-pair model, which is described as the ball of a point mass moving freely inside a 1D box and reflecting when hitting the boundary of the box. Due to the existence of the impacts, it has extremely complicated dynamical behavior, such as grazing bifurcation, singularity, and chaotic attractor [16–19]. The second is that a proper approach to studying VI systems is to attempt to establish its discrete Poincaré map (sometimes called the first return map). However, this map usually cannot be solved explicitly, thereby presenting the main difficulty with obtaining further analytical results.

Recently, a new type of VI-EH device was proposed in [20–22]. The device consists of a forced cylinder and a ball that moves freely inside the cylinder. Both ends of the cylinder are covered with membranes consisting of DE material that is sandwiched between two compliant electrodes, thereby acting as a variable capacitance capacitor. The principle of EH is that the ball impacts against one of the membranes and causes it to deform, resulting in a change in capacitance between the initial and deformed states, leading to EH. Thus, the kinetic energy is converted through the impacts of the potential energy of the deformed membrane, and then into electrical energy. Here, we consider a VI-EH system described as a small ball rolling inside a forced cylindrical capsule that is reflected after hitting the capsule ends. The main contribution of this paper is that we prove that the structure of the system is not destroyed by the impact of the ball. More precisely, in the nondissipative case, a proof of the existence of invariant curves is proved according to Moser’s twist theorem, which in turn proves that the kinetic energy of the ball is always bounded. Moreover, through the numerical simulation results, we find that in the nondissipative case, the energy of the ball is dissipative; i.e., infinite energy cannot also appear. Therefore, the structure of the system is not destroyed. The rest of this paper is organized as follows. In Section 2, we present a VI-EH and establish its Poincaré map. In Section 3, the existence of invariant curves is proved according to a version of Moser’s twist theorem. In Section 4, the global dynamical behavior of the system is investigated by numerical simulations, and the theoretical results are further verified. We draw the conclusions of this paper in Section 5.

2. Statement of the Problem

The VI-EH system can be modeled as a small ball of unitary mass rolling inside a forced cylindrical capsule that is inclined at a horizontal angle of β ($0 < \beta < \frac{\pi}{2}$), along with two DE membranes ∂B and ∂T for harvesting energy from ambient vibrations at the bottom and top of the capsule at distance L apart. The friction between the ball and the capsule is neglected, thus the motion of the ball is driven purely by impacts with one of the DE membranes and gravity. The elastic restitution coefficient for impacts between the ball and the DE membranes is $e \in (0, 1]$, and the mass of the capsule is huge with respect to the mass of the ball, which means that the impacts do not affect the motion of the capsule. Assume that the capsule moves periodically according to a C^6 and 1-periodic function $p(t)$, i.e., $p(t + 1) = p(t)$, see Figure 1.

Using the absolute coordinates, under the influence of the gravity and inclined angle, the motion of the ball moving inside the capsule satisfies as

$$\ddot{x} = -g \sin \beta, \quad (1)$$

where g is the gravitational acceleration. Assume that the motion equation of ∂B is

$$X(t) = p(t), \quad (2)$$

then, the motion equation of ∂T is $X(t) = p(t) + L$.

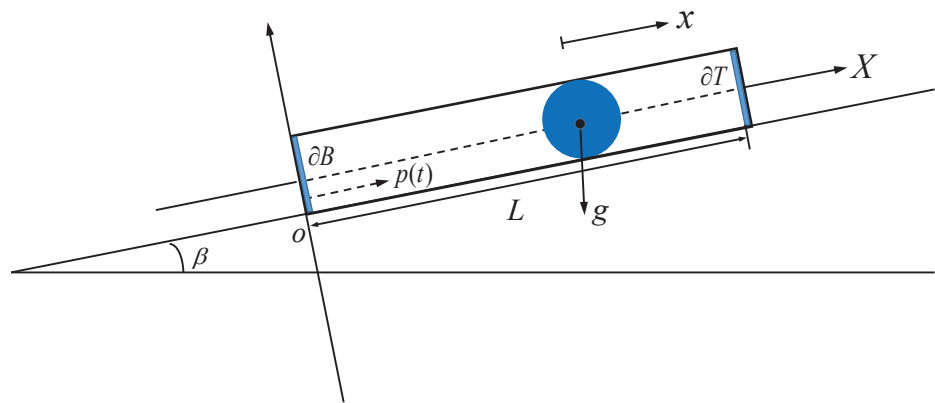


Figure 1. Schematic for vibro-impact energy harvesting (VI-EH) system.

Assuming that the impact occurs at instant τ , we consider the following problem

$$\begin{cases} \ddot{x} = -g \sin \beta, & p(t) \leq x(t) \leq p(t) + L, \\ x(\tau) = p(\tau) \text{ or } x(\tau) = p(\tau) + L \Rightarrow \dot{x}(\tau^+) = -e\dot{x}(\tau^-) + (1 + e)\dot{p}(\tau), \end{cases} \quad (3)$$

where $\dot{x}(\tau^+)$ and $\dot{x}(\tau^-)$ are the velocity of the ball before and after the impact at τ , respectively.

Remark 1. Note that the grazing and chattering phenomenons can also occur in this system, but we do not discuss them here because the research required to analyze them needs different approaches.

The problem (3) can usually be formulated in discrete form. Let $v = \dot{x}(t)$ denote the velocity of the ball. Suppose that at time t the ball impacts with ∂B and attains a velocity v after impact. Then, it moves from ∂B to ∂T and reaches ∂T at time \tilde{t} with the velocity \tilde{v} . After impact with ∂T , the ball attains a velocity \hat{v} . Continuing this process, the ball moves from ∂T to ∂B and reaches ∂T at time t' with the velocity \bar{v} . After impacts with ∂T , the ball attains a velocity v' . Based on the above analysis, we obtain

$$p(\tilde{t}) - p(t) + L = v(\tilde{t} - t) - \frac{g \sin \beta}{2}(\tilde{t} - t)^2 \quad (4)$$

and

$$\tilde{v} = v - \frac{g \sin \beta}{2}(\tilde{t} - t). \quad (5)$$

The relative velocity of the ball and ∂T before and after an impact is related by

$$\frac{\hat{v} - \dot{p}(\tilde{t})}{\tilde{v} - \dot{p}(\tilde{t})} = -e.$$

It gives

$$\hat{v} = -e\tilde{v} + (1 + e)\dot{p}(\tilde{t}). \quad (6)$$

Then, by (5) and (6), we have

$$\hat{v} = -ev + \frac{ge \sin \beta}{2}(\tilde{t} - t) + (1 + e)\dot{p}(\tilde{t}). \quad (7)$$

Completely similar to the above analysis, we have

$$p(\tilde{t}) - p(t') + L = -\bar{v}(t' - \tilde{t}) + \frac{g \sin \beta}{2}(t' - \tilde{t}) \quad (8)$$

and

$$\bar{v} = \hat{v} - \frac{g \sin \beta}{2}(t' - \tilde{t}). \tag{9}$$

The relative velocities of the ball and ∂B before and after an impact are related by

$$\frac{v' - \dot{p}(t')}{\bar{v} - \dot{p}(t')} = -e.$$

It gives that

$$v' = -e\bar{v} + (1 + e)\dot{p}(t'). \tag{10}$$

Then, we obtain from (8)–(10) that

$$\begin{aligned} v' &= -e\hat{v} + \frac{ge \sin \beta}{2}(\tilde{t} - t) - \frac{g \sin \beta}{2}(t' - \tilde{t}) + (1 + e)\dot{p}(t') \\ &= e^2v + \frac{ge \sin \beta}{2}(t' - \tilde{t} - e(\tilde{t} - t)) - (1 + e)(\dot{p}(t') - \dot{p}(\tilde{t})). \end{aligned} \tag{11}$$

A good strategy to describe the motion of the ball at the moments of impact with the same moving membranes ∂B (or ∂T) in problem (3) is to define a Poincaré map P that sends the couple (t, v) to (t', v') . In the following, we introduce a notion to construct the map P .

Define the sections

$$\Pi_1 = \{(x, v, t) \in \mathbb{R}^3 | x = X(t)\}$$

and

$$\Pi_2 = \{(x, v, t) \in \mathbb{R}^3 | x = X(t) + L\}.$$

Moreover, define the sections

$$\Lambda_1 = \{(t, v) | (p(t), v, t) \in \Pi_1\}$$

and

$$\Lambda_2 = \{(t, v) | (p(t) + L, v, t) \in \Pi_2\}.$$

The section Λ_1 (or Λ_2) can be interpreted as the Poincaré section. Thus, we obtain four basic maps $P_1 : \Lambda_1 \rightarrow \Lambda_2, P_2 : \Lambda_2 \rightarrow \Lambda_2, P_3 : \Lambda_2 \rightarrow \Lambda_1, P_4 : \Lambda_1 \rightarrow \Lambda_1$, which is defined by

$$\begin{aligned} P_1(t, v) &:= (t_0, v_0) &= (\tilde{t}, \tilde{v}), \\ P_2(t_0, v_0) &:= (t_1, v_1) &= (\tilde{t}, \hat{v}), \\ P_3(t_1, v_1) &:= (t_2, v_2) &= (t', \bar{v}), \\ P_4(t_2, v_2) &:= (t_3, v_3) &= (t', v'), \end{aligned}$$

respectively, see Figure 2.

Define the composition map $P = P_4 \circ P_3 \circ P_2 \circ P_1 : \Lambda_1 \rightarrow \Lambda_1$, and then P is regarded as a Poincaré map of problem (3).

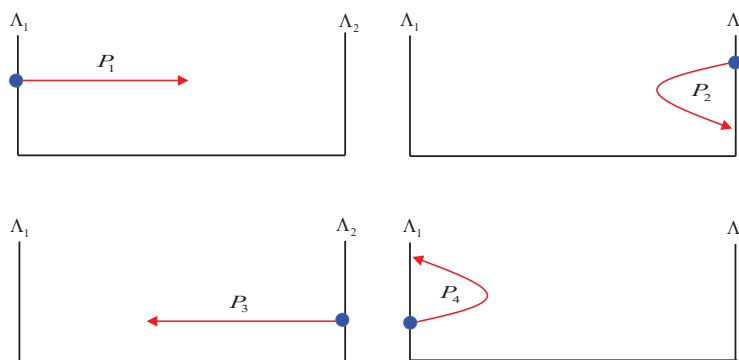


Figure 2. Schematic for four basic maps.

Lemma 1. The Poincaré map P has the expansion

$$\begin{cases} t' = t + \frac{L + (p(\tilde{t}) - p(t))}{v} + \frac{-L + (p(t') - p(\tilde{t}))}{\tilde{v}} + \mathcal{K}(g, \beta), \\ v' = e^2 v + \frac{g e \sin \beta}{2} (t' - \tilde{t} - e(\tilde{t} - t)) - (1 + e)(\dot{p}(t') - \dot{p}(\tilde{t})), \end{cases} \tag{12}$$

where

$$\begin{aligned} \mathcal{K}(g, \beta) &= \frac{-\alpha_1(p(\tilde{t}) - p(t) + L)}{v(2v + \alpha_1)} + \frac{\alpha_2(p(\tilde{t}) - p(t') + L)}{\tilde{v}(2\tilde{v} + \alpha_2)}, \\ \alpha_1 &= \frac{\mathcal{K}_1(g, \beta)}{\sqrt{v^2 + \mathcal{K}_1(g, \beta)} + v}, \quad \alpha_2 = \frac{\mathcal{K}_2(g, \beta)}{\sqrt{\tilde{v}^2 + \mathcal{K}_2(g, \beta)} + \tilde{v}}, \\ \mathcal{K}_1(g, \beta) &= -2g \sin \beta (p(\tilde{t}) - p(t) + L), \quad \mathcal{K}_2(g, \beta) = 2g \sin \beta (p(\tilde{t}) - p(t') + L). \end{aligned}$$

Proof. By (4), we have

$$\frac{g \sin \beta}{2} (\tilde{t} - t)^2 - v(\tilde{t} - t) + (p(\tilde{t}) - p(t) + L) = 0.$$

It gives

$$\begin{aligned} \tilde{t} - t &= \frac{2(p(\tilde{t}) - p(t) + L)}{v + \sqrt{v^2 - \frac{g \sin \beta}{2} (p(\tilde{t}) - p(t) + L)}} \\ &= \frac{p(\tilde{t}) - p(t) + L}{v} + \left(\frac{2(p(\tilde{t}) - p(t) + L)}{v + \sqrt{v^2 - \frac{g \sin \beta}{2} (p(\tilde{t}) - p(t) + L)}} - \frac{p(\tilde{t}) - p(t) + L}{v} \right). \end{aligned} \tag{13}$$

Then, we have

$$\tilde{t} - t = \frac{p(\tilde{t}) - p(t) + L}{v} + (p(\tilde{t}) - p(t) + L) \mathcal{Q}_1, \tag{14}$$

where

$$\begin{aligned} \mathcal{Q}_1 &= \frac{2}{v + \sqrt{v^2 - \frac{g \sin \beta}{2} (p(\tilde{t}) - p(t) + L)}} - \frac{1}{v} \\ &= \frac{2}{v + \sqrt{v^2 + \mathcal{K}_1(g, \beta)}} - \frac{1}{v} \\ &= \frac{-\mathcal{K}_1(g, \beta)}{v(2v + \sqrt{v^2 + \mathcal{K}_1(g, \beta)}) + \mathcal{K}_1(g, \beta)} \\ &= \frac{-1}{v(\frac{2v + \sqrt{v^2 + \mathcal{K}_1(g, \beta)}}{\mathcal{K}_1(g, \beta)} + 1)} = \frac{-\alpha_1}{v(2v + \alpha_1)} \end{aligned}$$

with $\mathcal{K}_1(g, \beta) := -2g \sin \beta (p(\tilde{t}) - p(t) + L)$ and $\alpha_1 = \frac{\mathcal{K}_1(g, \beta)}{\sqrt{v^2 + \mathcal{K}_1(g, \beta)} + v}$.

Similarly, we have

$$t' - \tilde{t} = \frac{-L + (p(t') - p(\tilde{t}))}{\tilde{v}} + (p(t') - p(\tilde{t}) - L)Q_2, \tag{15}$$

where $Q_2 = \frac{\alpha_2}{\tilde{v}(2\tilde{v} + \alpha_2)}$ with $\alpha_2 = \frac{\mathcal{K}_2(g, \beta)}{\sqrt{\tilde{v}^2 + \mathcal{K}_2(g, \beta) + \tilde{v}}}$, $\mathcal{K}_2(g, \beta) = 2g \sin \beta (p(\tilde{t}) - p(t') + L)$.

Thus, by (14) and (15), we get

$$t' = t + \frac{L + (p(\tilde{t}) - p(t))}{v} + \frac{-L + (p(t') - p(\tilde{t}))}{\tilde{v}} + \mathcal{K}(g, \beta),$$

where $\mathcal{K}(g, \beta) = (p(\tilde{t}) - p(t) + L)Q_1 + (p(\tilde{t}) - p(t') + L)Q_2$. \square

Lemma 2. *There is a sufficiently large constant $v^* > 0$ such that if the initial velocity $v > v^*$ and for every $t \in \mathbb{R}$, then the Poincaré map P is well defined and belongs to a class of functions of C^6 .*

Proof. By (12), we have

$$\tilde{t} - t = \frac{2(p(\tilde{t}) - p(t) + L)}{v + \sqrt{v^2 - \frac{g \sin \beta}{2}(p(\tilde{t}) - p(t) + L)}}. \tag{16}$$

Consider the function

$$F(\tilde{t}, t, v) = t' - t - \left(\frac{L + (p(\tilde{t}) - p(t))}{v} + \frac{-L + (p(t') - p(\tilde{t}))}{\tilde{v}} + \mathcal{K}(g, \beta) \right).$$

Then, for sufficiently large v , we have

$$\partial_{\tilde{t}} F(\tilde{t}, t, v) = 1 - O\left(\frac{1}{v}\right) > 0.$$

Thus, when v is large enough, for every couple (t, v) we get a unique $\tilde{t} = \tilde{t}(t, v)$ that satisfies Equation (16). By using the implicit function theorem, we obtain by uniqueness that $\tilde{t}(t, v)$ is a C^6 function. Then, by (12) we conclude that the Poincaré map P is well defined and belongs to a class of function of C^6 . \square

Remark 2. *Note that P is a 2D implicit map written in terms of the variables' energy and time when the ball leaves the moving capsule ends, which usually give rise to the main difficulties for analytical investigation.*

Lemma 3. *There exists a constant sufficiently large constant $v^* > 0$ and $t \in \mathbb{R}$ such that the Poincaré map P is an area-preserving map in the nondissipative case, i.e., the elastic restitution coefficient $e = 1$.*

Proof. When $r = 1$, by Lemma 1, the Poincaré map P is

$$\begin{cases} t' = t + \frac{L + (p(\tilde{t}) - p(t))}{v} + \frac{-L + (p(t') - p(\tilde{t}))}{\tilde{v}} + \mathcal{K}(g, \beta), \\ v' = v + \frac{g \sin \beta}{2}(t' - 2\tilde{t} + t) - 2\dot{p}(\tilde{t}) + 2\dot{p}(t'). \end{cases} \tag{17}$$

Let $X = p(t)$, $H(X, v) = v^2/2 + Xg \sin \beta$, $X_2 = p(t_1) + L = p(t_2) + L$, $X_3 = X_4 = p(t_3) = p(t_4)$. For the maps P_1 and P_3 , the integral invariant of Poincaré–Cartan (c.f. [23]) yields

$$\begin{aligned} \oint_{\Gamma} v dX - H(X, v) dt &= \oint_{P_1(\Gamma)} v_1 dX_1 - H(X_1, v_1) dt_1, \\ \oint_{P_2 \circ P_1(\Gamma)} v_2 dX_2 - H(X_2, v_2) dt_2 &= \oint_{P_3 \circ P_2 \circ P_1(\Gamma)} v_3 dX_3 - H(X_3, v_3) dt_3, \end{aligned} \tag{18}$$

where $\Gamma = \{(t, \mu(t)) : t \in \mathbb{R}, \mu(t) > v^*\}$ is any a C^1 Jordan curve in the definition region P .
 Set $dX = \dot{p}(t)dt, dX_1 = dX_2 = \dot{p}(t_1)dt_1 = \dot{p}(t_2)dt_2, dX_3 = \dot{p}(t_3)dt_3$. This transforms Equation (18) to

$$\begin{aligned} \oint_{\Gamma} (v\dot{p}(t)dt - \frac{v^2}{2} - p(t)Xg \sin \beta)dt &= \oint_{P_1(\Gamma)} (v_1\dot{p}(t_1)dt_1 - \frac{v_1^2}{2} - p(t_1)X_1g \sin \beta)dt_1, \\ \oint_{P_2 \circ P_1(\Gamma)} (v_2\dot{p}(t_2)dt_2 - \frac{v_2^2}{2} - p(t_2)X_2g \sin \beta)dt_2 &= \oint_{P_3 \circ P_2 \circ P_1(\Gamma)} (v_3\dot{p}(t_3)dt_3 - \frac{v_3^2}{2} - p(t_1)X_3g \sin \beta)dt_3. \end{aligned} \tag{19}$$

Taking into account both (7) and (8), we obtain

$$\begin{aligned} \oint_{P_1(\Gamma)} (v_1\dot{p}(t_1)dt_1 - \frac{v_1^2}{2} - p(t_1)X_1g \sin \beta)dt_1 &= \oint_{P_2 \circ P_1(\Gamma)} (v_2\dot{p}(t_2)dt_2 - \frac{v_2^2}{2} - p(t_2)X_2g \sin \beta)dt_2, \\ \oint_{P_3 \circ P_2 \circ P_1(\Gamma)} (v_3\dot{p}(t_3)dt_3 - \frac{v_3^2}{2} - p(t_1)X_3g \sin \beta)dt_3 &= \oint_{P(\Gamma)} (v'\dot{p}(t')dt' - \frac{v'^2}{2} - p(t')X'g \sin \beta)dt'. \end{aligned} \tag{20}$$

From (19) and (20), we get

$$\oint_{\Gamma} (v\dot{p}(t) - \frac{v^2}{2} - p(t)g \sin \beta)dt = \oint_{P(\Gamma)} (v'\dot{p}(t') - \frac{v'^2}{2} - p(t')g \sin \beta)dt'. \tag{21}$$

It is obvious that the curves Γ and $P(\Gamma)$ either intersect or one of them goes around the other. Suppose that the later case occurs and let \mathcal{R} denote the domain that is bounded by Γ and $P(\Gamma)$. When v is sufficiently large, by Green’s formula (c.f. [23]) and (21), we have $\iint_{\mathcal{R}} (\dot{p}(t) - v)dt dv = 0$. In fact, when v^* is sufficiently large, we also have $\iint_{\mathcal{R}} (\dot{p}(t) - v)dt dv < 0$. This naturally leads to a contradiction; thus, the intersection of the curves Γ and $P(\Gamma)$ is nonempty (called Moser’s intersection property) and the Poincaré map P is an area-preserving map. \square

3. The Existence of Invariant Curves

In this section, a proof of the existence of invariant curves for the system is given, based on Moser’s twist theorem in the nondissipative case. To illustrate the main results below, we first briefly review some of the definitions and results of Moser’s twist theorem investigations into area-preserving maps [23–25].

By [26], we know that an irrational number α is said to be a type of constant γ . If γ is defined by

$$\gamma = \inf \left\{ q^2 \left| \alpha - \frac{p}{q} \right| : p, q \in \mathbb{Z}, q \geq 1 \right\}$$

then it is strictly positive and γ is called the Markoff constant of α .

Lemma 4. *In choosing a 1D interval $[a, b] \subset [0, 1]$ with $b - a \geq \varepsilon > 0$ on the real-number axial, there exists a constant type $\alpha \in [a, b]/\mathbb{Q}$ such that the corresponding Markoff constant satisfies $\frac{\varepsilon}{16} \leq \gamma \leq \frac{\varepsilon}{4}$.*

Theorem 1. *(Moser’s twist theorem) Assume that the operator $\Phi : \mathbb{R} \times [-1, 1] \rightarrow \mathbb{R} \times \mathbb{R}$ is a diffeomorphism that belongs to a class of functions of C^5 and is a 1-periodic function with respect to the variable θ . Moreover, assume that the specific form of Φ is*

$$\begin{cases} \theta' = \theta + \alpha + \delta r + \delta \varphi(\theta, r), \\ r' = r + \delta \phi(\theta, r), \end{cases} \tag{22}$$

where $0 < \delta < 2$ and α is an irrational number of constant type with Markoff constant γ , thereby satisfying

$$\gamma \leq \delta \leq b\gamma \tag{23}$$

for some fixed b . We also assume that the operator Φ has Moser’s intersection property (see the proof of Lemma 2.3), i.e., for any parameterized C^1 Jordan curve $\Gamma = \{(\theta, \mu(\theta)) : \theta \in \mathbb{R}\}$ located in region $\mathbb{R} \times [-1, 1]$ that satisfies $\Gamma \cap \Phi(\Gamma) \neq \emptyset$, there is a positive constant C that depends only on fixed b , such that if

$$\|\varphi(\theta, r)\|_{C^5} + \|\phi(\theta, r)\|_{C^5} \leq C,$$

then there exists $\mu \in C^3(\mathbb{S}^1)$ such that $\Gamma = \{\theta, \mu(\theta) : \theta \in \mathbb{R}\}$ is invariant under the action of operator Φ , and the rotation number of $\Phi|_\Gamma$ is α .

Remark 3. The proofs of Lemma 3.1 and Theorem 3.1 were given in [26,27], respectively, so we do not repeat them. These theories were applied to the study of different dynamical systems, such as breathing circle billiard [28], piece-wise linear oscillator [29], and so on.

We are now ready to prove the main result of this paper, say

Theorem 2. There exists a constant number $\kappa > 0$ such that if the function p satisfies

$$\left| \frac{d^k p(t)}{dt^k} \right| < \kappa, \quad \forall t \in \mathbb{R}, k = 0, 1, \dots, 6,$$

then there exist curves $\Gamma = \{(t, \mu(t)) : t \in \mathbb{R}\}$ with $\mu \in C^3(\mathbb{S}^1)$ that are invariant under the Poincaré map P , resulting in the energy of the ball always being bounded.

Proof. Let

$$\begin{cases} \mathcal{F}(t, v) = \frac{-L + (p(t') - p(\tilde{t}))}{\tilde{v}} + \mathcal{K}(g, \beta), \\ \mathcal{G}(t, v) = \frac{g \sin \beta}{2} (t' - 2\tilde{t} + t) - 2\dot{p}(\tilde{t}) + 2\dot{p}(t'). \end{cases}$$

Then, by (17), the map P has the expansion

$$\begin{cases} t' = t + \frac{L + (p(\tilde{t}) - p(t))}{v} + \mathcal{F}(t, v), \\ v' = v + \mathcal{G}(t, v). \end{cases}$$

By Lemma 4, we get a sequence $\{\alpha_n\}$ of irrational numbers of constant type converging to 0, and this satisfies

$$\frac{1}{2n} \leq \alpha_n \leq \frac{1}{n}, \quad \frac{1}{32n} \leq M_n \leq \frac{1}{8n}.$$

Define ε_n by $\alpha_n = \frac{4(L+(p(\tilde{t})-p(t)))}{n\varepsilon_n}$ and consider transformation

$$U_n : \left(\theta, \frac{n\varepsilon_n}{r+4}\right) \mapsto (t, v).$$

The transformation U_n maps the region $D = \{(\theta, r) : \theta \in \mathbb{R}, r \in [-1, 1]\}$ to the region $D_n = \{(t, v) : t \in \mathbb{R}, v \in [\frac{n\varepsilon_n}{5}, \frac{n\varepsilon_n}{3}]\}$. Since $n\varepsilon_n = \frac{4(L+(p(\tilde{t})-p(t)))}{\alpha_n}$, the distance from the region D_n to the line $v = 0$ goes to infinity when $n \rightarrow \infty$. Let

$$P_n = U_n^{-1} \circ P \circ U_n : D \rightarrow \mathbb{R}^2.$$

We obtain

$$P_n : \begin{cases} \theta' = \theta + \alpha_n + \delta_n r + \delta_n \phi_n(\theta_n, r_n), \\ r' = r + \delta_n \phi_n(\theta_n, r_n), \end{cases}$$

where $\delta_n = \frac{\alpha_n}{4}$, $\phi_n(\theta_n, r_n) = \frac{1}{\delta_n} \mathcal{F}\left(\theta, \frac{n\varepsilon_n}{r+4}\right)$, $\phi_n(\theta_n, r_n) = \mathcal{G}\left(\theta, \frac{n\varepsilon_n}{r+4}\right) \frac{(r+4)^2(L+p(\bar{t})-p(t))^{-1}}{1+\mathcal{G}\left(\theta, \frac{n\varepsilon_n}{r+4}\right)(r+4)^{n-1}\varepsilon_n^{-1}}$.

Since the map P satisfies the Moser’s intersection property (see the proof of Lemma 3) and P_n is homeomorphic to P , we can conclude that P_n also satisfies Moser’s intersection property. Since (23) holds for $b = 8$, then we can apply Theorem 1 as soon as both $\|\varphi(\theta, r)$ and $\|_{C^5}, \|\phi(\theta, r)\|_{C^5}$ are sufficiently small. The case is held because we chose an n that is sufficiently large and assumed that $\|p\|_{C^6}$ is sufficiently small. Thus, by Theorem 1, P_n has an invariant curve. We then obtain a curve $\Gamma_n = \{(t, \mu_n(t)) : t \in \mathbb{R}\}$ with $\mu_n \in C^3(\mathbb{S}^1)$ via the transformation U_n , which is also invariant under the action of P . After passing to a subsequence $\{\mu_n\}_{n \geq 1}$, we assume that $\mu_n(t) \leq \mu_{n+1}(t)$ and $\lim_{n \rightarrow \infty} \mu_n(t) = \infty$ uniformly with respect to $t \in \mathbb{R}$. Define a region

$$B_n = \{(t, v) : t \in \mathbb{R}, \mu_n(t) \leq v \leq \mu_{n+1}(t)\}$$

for $n \geq 1$. The region B_n is homomorphically mapped to its image by P , and the boundary of B_n is invariant. Thus, B_n must be invariant under the action of P . Let v^* be a constant such that $\{(t, v) : v \geq v^*\} \subset \cup_{n \geq 1} B_n$. When $v \geq v^*$, it follows that $(t, v) \in B_N$ for some $N \geq 1$. By invariance of B_N , the orbit $\{P^n(t, v)\}$ is completely contained in B_N . Therefore, we conclude that $\{P^n(t, v)\}$ is bounded, i.e., the energy of the ball is bounded. \square

Remark 4. According to Theorem 3.2, the existence of invariant curves also provides the stability results of the problem (3): if the initial condition of the system is on an invariant curve, then the future dynamical evolution will stay confined to that invariant curve forever; if the initial condition of the system lies between two invariant curves, the future dynamical evolution will stay bounded between them forever. Moreover, the existence of invariant curves also ensures that the kinetic energy of the ball is always bounded, and hence, the structure of VI-EH is not destroyed by the impact of the ball.

Remark 5. The symmetry of the system is mainly reflected in two aspects: on the one hand, it refers to the geometric symmetry of the system; on the other hand, it refers to the symmetry of the dynamical behavior of the system. The geometric symmetry is obvious. If the DE materials covered in both ends of the cylinder capsule are different, that is, the restitution coefficients of the collisions are different, then the dynamic behavior of the system is asymmetric (see [30] for a similar analysis). If the restitution coefficients of the collisions are the same and $p(t)$ is chosen as a class of specific functions that satisfies $p(t + n/2) = -p(t)$ (n is odd integer), then the Poincaré map P of problem (3) has the property of symmetry, such that if Γ is an invariant curve of P , then $P(\Gamma)$ is also an invariant curve of P (c.f. [31,32]).

Remark 6. If $\beta = 0$, then the cylindrical capsule moves along the horizontal direction, and Theorem 2 still holds in this case.

4. Numerical Simulations

In this section, we discuss the numerical simulations results obtained from the VI-EH system to further verify our theoretical results. We first discuss the dynamical behavior of the system in the nondissipative case, and then discuss the dissipative case.

Choose $p(t) = \zeta \sin t, \zeta = 0.1, \beta = \pi/8, e = 1, L = 6$ m and v change from 50 m/s to 52 m/s. We find that the system exhibits regular dynamic behavior, mainly containing periodic points (Birkhoff type), invariant curves, and Aubry–Mather sets (the definition of Aubry–Mather sets can be found in [33]), see Figure 3. Moreover, the existence of invariant curves also ensures that the kinetic energy of the ball is always bounded. For the same

parameter condition, i.e., only choosing $v = 52$ m/s, $e = 0.99$, the dissipation introduced by the coefficient of restitution e destroys the regular dynamic behavior in the nondissipative case and generates a low-energy periodic point, see Figure 4.

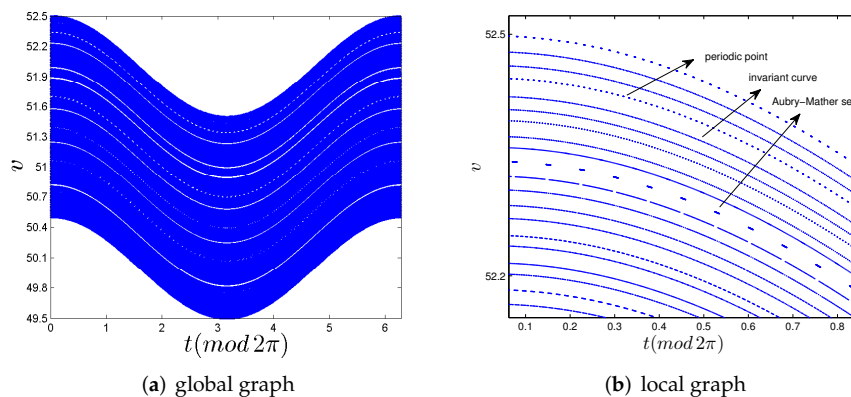


Figure 3. Regular dynamic behavior containing periodic points, invariant curves, and Aubry–Mather sets.

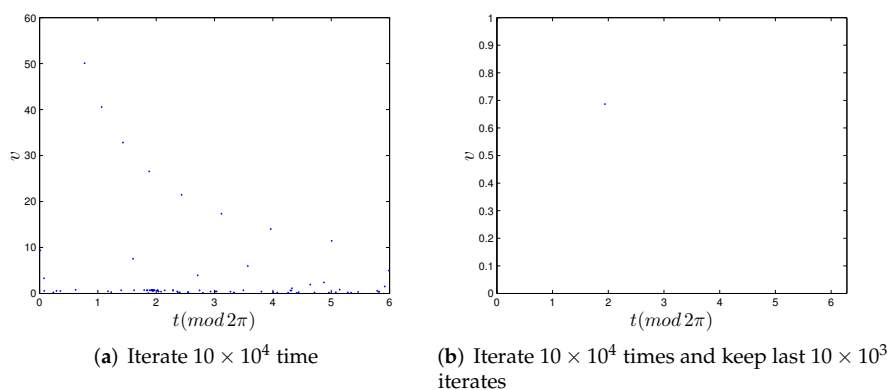


Figure 4. A low-energy periodic point.

5. Conclusions

In this work, we consider a two-sided vibro-impact energy harvester (VI-EH) system. Our main objective is to investigate whether the structure of the system will be destroyed by the impact of the ball. For this objective, we study the nondissipative and dissipative cases of the system, respectively. We show that the dynamics of the system are described by the use of a 2D implicit map, and the existence of invariant curves in the nondissipative case is proved by using Moser’s twist theorem. Thus, in nondissipative case, the kinetic energy of the ball is always bounded, and the structure of system is not destroyed by the impacts of the ball. Furthermore, by numerical analysis we also obtain that the dynamical behavior of this system is regular. After the introduction of dissipation, the dissipation destroys the regular dynamical behavior in the nondissipative case, and a periodic point with low energy appears. In summary, the structure of the system was not destroyed, and the theoretical analysis shows that this is mainly related to the smoothness of the system.

Author Contributions: Z.C. and X.Y.: writing—original draft preparation; H.M. and H.Y.: methodology; J.S.: software; Y.T. and G.R.: formal analysis and investigation. All authors have read and agreed to the published version of the manuscript.

Funding: This work is supported by the National Natural Science Foundations of China (12172306 and 11732014).

Institutional Review Board Statement: Not applicable.

Informed Consent Statement: Not applicable.

Data Availability Statement: All data used during the study appear in the submitted article.

Conflicts of Interest: The authors declare no conflict of interest.

References

1. Daqaq, M.F.; Masana, R.; Erturk, A.; Quinn, D.D. On the role of nonlinearities in vibratory energy harvesting: a critical review and discussion. *Appl. Mech. Rev.* **2014**, *66*, 040801. [[CrossRef](#)]
2. Yang, Z.; Zhou, S.; Zu, J.; Inman, D. High-performance piezoelectric energy harvesters and their applications. *Joule* **2018**, *2*, 642–697. [[CrossRef](#)]
3. Carneiro, P.; dos Santos, M.P.S.; Rodrigues, A.; Ferreira, J.A.; Simões, J.A.; Marques, A.T.; Kholkin, A.L. Electromagnetic energy harvesting using magnetic levitation architectures: A review. *Appl. Energy* **2020**, *260*, 114191. [[CrossRef](#)]
4. Thomson, G.; Lai, Z.; Val, D.; Yurchenko, D. Advantages of nonlinear energy harvesting with dielectric elastomers. *J. Sound Vib.*, **2019**, *442*, 167–182. [[CrossRef](#)]
5. Zhao, H.; Ouyang, H. A capsule-structured triboelectric energy harvester with stick-slip vibration and vibro-impact. *Energy* **2021**, *235*, 121393. [[CrossRef](#)]
6. Bowen, C.; Kim, A.; Weaver, P.; Dunn, S. Piezoelectric and ferroelectric materials and structures for energy harvesting applications. *Energy Environ. Sci.* **2014**, *7*, 25–44. [[CrossRef](#)]
7. Salazar, R.; Larkin, K.; Abdelkefi, A. Piezoelectric property degradation and cracking impacts on the lifetime performance of energy harvesters. *Mech. Syst. Signal Process* **2021**, *156*, 107697. [[CrossRef](#)]
8. Alevras, P.; Theodossiades S.; Rahnejat H. Broadband energy harvesting from parametric vibrations of a class of nonlinear Mathieu systems. *Appl. Phys. Lett.* **2017**, *110*, 233901. [[CrossRef](#)]
9. Xia, G.; Fang, F.; Zhang, M.; Wang, Q.; Wang, J. Performance analysis of parametrically and directly excited nonlinear piezoelectric energy harvester. *Arch. Appl. Mech.* **2019**, *89*, 2147–2166. [[CrossRef](#)]
10. Nabholz, U.; Lamprecht, L.; Mehner, J.; Zimmermann, A.; Degenfeld-Schonburg, P. Parametric amplification of broadband vibrational energy harvesters for energy-autonomous sensors enabled by field-induced striction. *Mech. Syst. Signal Process* **2020**, *139*, 106642. [[CrossRef](#)]
11. Wang, J.; Geng, L.; Zhou, S.; Zhang, Z.; Lai, Z.; Yurchenko, D. Design, modeling and experiments of broadband tristable galloping piezoelectric energy harvester. *Acta Mech. Sin.* **2020**, *36*, 592–605. [[CrossRef](#)]
12. Fu, H.; Mei, X.; Yurchenko, D.; Zhou, S.; Nakano, K.; Yeatman, E. Rotational energy harvesting for self-powered sensing. *Joule* **2021**, *5*, 1074–1118 [[CrossRef](#)]
13. Fang, S.; Zhou, S.; Yurchenko, D.; Yang, T.; Liao, W. Multistability phenomenon in signal processing, energy harvesting, composite structures, and metamaterials: A review. *Mech. Syst. Signal Process* **2022**, *166*, 108419. [[CrossRef](#)]
14. Fu, Y.; Ouyang, H.; Davis, R. Triboelectric energy harvesting from the vibro-impact of three cantilevered beams. *Mech. Syst. Signal Process* **2019**, *121*, 509–531. [[CrossRef](#)]
15. Cao, D.; Xia, W.; Guo, X.; Lai, S. Modeling and experiment of vibro-impact vibration energy harvester based on a partial interlayer-separated piezoelectric beam. *J. Intell. Mater. Syst. Struct.* **2021**, *32*, 817–831. [[CrossRef](#)]
16. Zhang, Y.; Fu, X. Stability of periodic motions in an inclined impact pair. *Eur. Phys. J. Spec. Top.* **2019**, *228*, 1441–1457. [[CrossRef](#)]
17. Fu, X.; Zhang, Y. Stick motions and grazing flows in an inclined impact oscillator. *Chaos Solitons Fractals* **2015**, *76*, 218–230. [[CrossRef](#)]
18. Luo, A.; Guo, Y. *Vibro-Impact Dynamics*; John Wiley & Sons Ltd.: Oxford, UK, 2013.
19. Luo, A. Period-doubling induced chaotic motion in the LR model of a horizontal impact oscillator. *Chaos Soliton. Fract.* **2004**, *19*, 218–230. [[CrossRef](#)]
20. Yurchenko, D.; Lai, Z.; Thomson, G.; Val, D.; Bobryk, R. Parametric study of a novel vibro-impact energy harvesting system with dielectric elastomer. *Appl. Energy* **2017**, *208*, 456–470. [[CrossRef](#)]
21. Serdukova, L.; Kuske, R.; Yurchenko, D. Stability and bifurcation analysis of the period-T motion of a vibroimpact energy harvester. *Nonlinear Dyn.* **2019**, *98*, 1807–1819. [[CrossRef](#)]
22. Yurchenko, D.; Val, D.; Lai, Z.; Thomson, G. Energy harvesting from a DE-based dynamic vibro-impact system. *J. Smart Mater. Struct.* **2017**, *26*, 105001. [[CrossRef](#)]
23. Arnold, V.; Kozlov, V.; Neishtadt, A. *Mathematical Aspects of Classical and Celestial Mechanics*; Springer: Berlin/Heidelberg, Germany, 1997.
24. Katok, A.; Hasselblatt, B. *Introduction to the Modern Theory of Dynamical Systems*; Cambridge University Press: Cambridge, UK, 1995.
25. Moser, J. *Selected Chapters in the Calculus of Variations*; Birkhäuser: Boston, MA, USA, 2003.
26. Ortega, R. Asymmetric oscillators and twist mappings. *J. Lond. Math. Soc.* **1996**, *53*, 325–342. [[CrossRef](#)]
27. Herman, M. Sur les courbes invariantes par les difféomorphismes de l’anneau. *Astérisque* **1983**, *103–104*, 1–221.
28. Zhang, X.; Xie, J.; Li, D.; Cao, Z.; Grebogi, C. Stability analysis of the breathing circle billiard. *Chaos Soliton. Fract.* **2021**. doi.org/10.1016/j.chaos.2021.111643. [[CrossRef](#)]

29. Ortega, R. Boundedness in a piecewise linear oscillator and a variant of the small twist theorem. *Proc. Lond. Math. Soc.* **1999**, *79*, 381–413. [[CrossRef](#)]
30. Dulin, S.; Lin, K.; Serdukova, L.; Kuske, R.; Yurchenko, D. Improving the performance of a two-sided vibro-impact energy harvester with asymmetric restitution coefficients. *Int. J. Mech. Sci.* **2022**, *217*, 106983. [[CrossRef](#)]
31. Cao, Z.; Zhang, X.; Li, D.; Yin, S.; Xie, J. Existence of invariant curves for a Fermi type impact absorber. *Nonlinear Dyn.* **2020**, *99*, 2647–2656. [[CrossRef](#)]
32. Yue, Y.; Xie, J. Symmetry and bifurcations of a two-degree-of-freedom vibro-impact system. *J. Sound Vib.* **2008**, *314*, 228–245. [[CrossRef](#)]
33. Cao, Z.; Grebogi, Z.; Li, D.; Yue, Y.; Xie, J. On the global dynamical properties of a Fermi-Ulam model. *Differ. Equ. Appl.* **2021**, *27*, 1647–1656. [[CrossRef](#)]